J. Biochem. **143,** 339–347 (2008)
doi:10.1093/jb/mvm225

Recognition of a Bulged RNA by Peptides Derived from the Influenza NS1 Protein

Tatsuhiko Someya*,†, Kazumi Hosono†, Kaori Morimura, Hiroshi Takaku and Gota Kawai‡

Department of Life and Environmental Sciences, Faculty of Engineering, Chiba Institute of Technology, 2-17-1 Tsudanuma, Narashino-shi, Chiba 275-0016, Japan

Received August 27, 2007; accepted November 12, 2007; published online November 26, 2007

A competition assay for RNA binding by the influenza virus NS1 protein using model RNAs, U6–45, corresponding to U6 snRNA revealed that deletion of each of the three bulged-out parts reduced the NS1 protein binding and, in contrast, by deleting all three of the bulged-out parts, simultaneously, and thus producing a double-stranded RNA, the binding was recovered. A common feature of target RNAs of the NS1 protein, U6 snRNA, poly(A) and viral RNA, is the stretch of 'bulged-out' A residues. Thus, the NS1 protein was found to recognize either the stretch of 'bulged-out' A residues or dsRNA which is also a target of the NS1 protein. Furthermore, a basic peptide, NS1–2, derived from the helix-2 of the RNA binding site of NS1 protein was designed and its binding to the U6 snRNA was analysed by using a model RNA for U6 snRNA, U6–34. The NMR signals due to H8/H6 and H1′ of U6–34 were assigned and their changes upon binding of NS1–2 were analysed. It was indicated that NS1–2 interacts with the residues in the bulge-out region of U6–34. These results suggest that NS1–2 recognizes the U6 snRNA in a similar manner to NS1 protein.

Key words: gel shift, influenza virus, NMR, NS1 protein, RNA-binding protein, U6 snRNA.

Abbreviations: dsRNA, double-stranded RNA; PAGE, polyacrylamide gel electrophoresis; NS1, non-structural protein 1; snRNA, small nuclear RNA.

Non-structural protein 1 (NS1) of influenza virus type A, consisting of 202–237 amino acid residues, is encoded on the smallest segment, the eighth segment, and forms a homo-dimer (*1–5*). The NS1 protein consists of at least two functional domains: the RNA-binding domain, located on the N-terminal half, and the effector domain (*6*). Between the two domains, an eIF4GI-binding domain was also found (*7*). The NS1 protein affects several steps of host translation, including the inhibition of nuclear export of mature cellular mRNA by binding to the 3′ poly(A) tail (*8*), and the inhibition of mRNA splicing by binding to the U6 snRNA and U6atac snRNA (*9–11*). The NS1 protein also binds to double-stranded RNA (dsRNA) (*12*, *13*), which inhibits the antiviral activity of the IFN-α/β-induced 2′-5′-oligo(A) synthetase/RNase L pathway (*14*). Furthermore, the NS1 protein binds to viral RNAs (*15–17*) and increases their translation level in combination with binding to eIF4GI (*7*). Thus, NS1 protein binding to different kinds of RNA with various sequences and structures is important for its function.

The solution and crystal structures of an RNA binding domain of NS1 protein, NS1(1–73), have been reported (*18*, *19*). The NS1(1–73) consists of the amino acid residues 1–73 of the NS1 protein, and forms a dimer with the same RNA-binding activity as the full-length protein (*5*). The NS1(1–73) protein monomer was found to consist of three α-helices, with no β-sheets (Fig. 1A). U6 snRNA is one of the members of small nuclear RNAs, and interacts with U2 and U4 snRNA during the pre-mRNA splicing reaction (for review, see *20*).

Mutagenesis experiments suggested that RNA binding requires the dimer formation and the arginine residue at position 38 and the lysine residue at position 41, both of which are located in the second helix of each monomer, are the only amino acid residues that are absolutely required only for RNA binding, but not for the dimerization (*18*). However, the mechanism of the binding of NS1 protein to its RNA targets is still not known.

Figure 2A shows the secondary structure of human U6 snRNA (*21*, *22*). The NS1 protein-binding site was reported to be in the range of residues 37–43 and 88–95 including the 5 bulge-out residues by Qin, Y. *et al*. (*10*). This region was shown to include a stem structure by Harada *et al* (*21*) as shown in Fig. 2A whereas Rinke *et al*. (*22*) showed that the region forms an internal loop structure.

In the present study, to analyse the RNA binding properties of the NS1 protein, the affinity of its RNA binding domain to model RNAs, U6–45 corresponding to the U6 snRNA (Fig. 2B), was analysed by a competitive gel shift assay *in vitro*. Our results indicate that the NS1 protein recognizes either the stretch of 'bulged-out' A residues or dsRNA. Furthermore, we also designed two

*Present address: Graduate School of Life and Environmental Sciences, University of Tsukuba, 1-1-1 Tennodai, Tsukuba-shi, Ibaraki 305-8572, Japan.
†These authors contribute to this work equally.
‡To whom correspondence should be addressed. Fax: +81-47-478-0425, E-mail: gkawai@sea.it-chiba.ac.jp

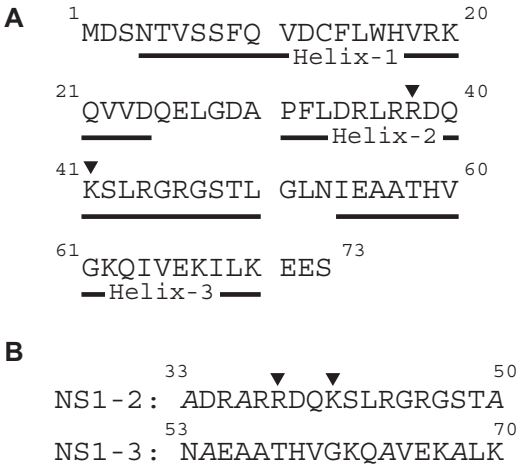

Fig. 1. **Amino acid sequence of a protein and peptides used in this study.** Amino acid sequence of the RNA binding domain of NS1 protein is shown with the position of the three α-helices indicated by underlines (A). Residues involved in direct RNA binding, Arg38 and Lys41, are indicated by arrowheads (*26*). The mutant peptides were derived from the helices-2 and -3 of the RNA-binding domain and three hydrophobic residues are replaced by alanine, indicated by italic font, for each peptide (B).

peptides derived from NS1 protein; NS1–2 and NS1–3 correspond to the helices -2 and -3, respectively (Fig. 1B). For each peptide, some hydrophobic residues are replaced by alanine residues to increase the water solubility. The gel shift assay using these peptides and a shorter model RNA, U6–34 (Fig. 2C) indicated that the short peptide NS1–2 possesses the RNA binding activity. It was confirmed by NMR experiments that NS1–2 binds to the bulge-out region of U6–34.

MATERIALS AND METHODS

Preparation of the Influenza NS1 Protein and Related Peptides—The influenza NS1 protein (A/PR/8/34 strain) was overproduced and fractionated essentially as described by Young *et al.* (*23*), except that the host strain for the expression plasmid pAS-NS (a gift from Dr S. Nakata) was *Escherichia coli* strain N4830-1 (Amersham Pharmacia Biotech). We added an extra purification step, involving anion-exchange column chromatography, with a linear gradient of 50–200 mM NaCl in 40 mM Tris–HCl (pH 8.0). The purity of NS1 protein was analysed by 15% SDS–PAGE using Coomassie Brilliant Blue staining. Peptide samples were purchased from Sawady Technoloty Co. Ltd.

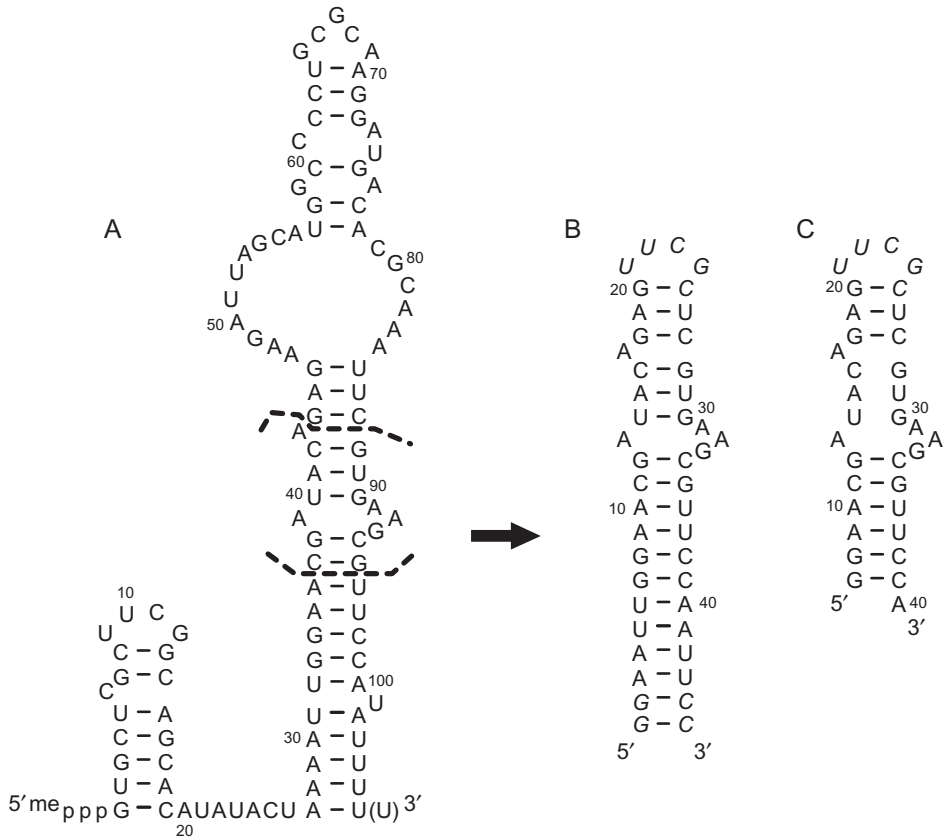

Fig. 2. **Secondary structures of human U6 snRNA (A) and model RNAs, U6–45 (B), and U6–34 (C).** The NS1 binding site of human U6 snRNA is indicated by broken lines according to Qin *et al.* (*10*). U6–45 was designed to include the NS1 binding site. The two strands were connected with the stable UUCG loop, and the terminal base pairs were changed to GC pairs to increase the production yield for *in vitro* transcription by using the T7 RNA polymerase. A model RNA, U6–34, includes the NS1 protein binding site (C). Two strands were also connected with the stable UUCG loop, and the GU base pair closing the UUCG loop was changed to a GC pair. These modifications are indicated by italic font. The residue number is defined for U6–45, which does not correspond to that of U6 snRNA for convenience. The secondary structure of U6–34 reflected the result of the present NMR analysis.

Preparation of RNA Samples—5′-fluorescein-labelled U6–45 RNAs were chemically synthesized with a DNA/RNA synthesizer (Expedite 8909, Perseptive) using fluorescein phosphoramidite (Glen Research). After deprotection, the 5′-fluorescein-labelled RNAs were purified using 20% polyacrylamide gel electrophoresis (PAGE) under denaturing conditions with 8 M urea, and extensively desalted by ultrafiltration. Non-labelled U6–45 and its mutant RNAs were also synthesized by the same method.

For NMR measurements, U6–34 RNAs were enzymatically synthesized by an *in vitro* transcription reaction using T7 RNA polymerase. To improve the resolution of NMR signals, semi-selective [^{13}C, ^{15}N] labelling was introduced to A/U, A, G and C using [*U*-^{13}C,^{15}N]NTPs (Taiyo Nippon Sanso). The transcripts were purified by 15% PAGE under denaturing conditions with 7 M urea, and extensively desalted by ultrafiltration.

For purified RNA samples were annealed by heating at 95°C for 5 min and snap-cooling on ice. The formation of the hairpin structure for each RNA sample was confirmed by PAGE under native condition.

RNase Probing Analyses—For the RNA digestion reaction, 5′-fluorescein-labelled RNA (0.1 μM) was used. RNA samples were dissolved in 20 mM Tris–HCl (pH 7.8), 5 mM $MgCl_2$, 100 mM NaCl and 1 mM dithiothreitol. The reactions were carried out on ice for 5–15 min in the presence of 1, 6 and 0.02 units of RNase T_1, T_2 and V_1, respectively. The digests were analysed by 20% PAGE with an acrylamide:bis ratio of 19:1, in 80 mM Tris–borate (pH 8.3), 2 mM EDTA and 8 M urea, and a plate size of 200 × 400 mm. Detection and analysis of RNAs were performed using the gel analysis system, FLA-2000G (Fuji Photo Film Co., Ltd).

Competitive Gel Shift Assay—The 5′-fluorescein-labelled RNA was mixed with the NS1 protein in the presence of various concentration of non-labelled RNA, and the formation of a labelled RNA-NS1 protein complex was analysed by PAGE under the native condition. Prior to PAGE analysis, samples were mixed in binding buffer containing 5 mM Tris–HCl (pH 7.8), 50 mM KCl, 8% glycerol and 1 mM dithiothreitol, and were incubated at 4°C for 30 min. The sample concentrations in the binding buffer were 0.05 μM for labelled RNA, 0.12 μM for the NS1 protein as the monomer and 0–1 μM for non-labelled RNA. The NS1-protein bound RNAs were separated from the unbound RNA by 6% PAGE with acrylamide:bis ratio of 59:1, in 20 mM Tris–borate (pH 8.3), 0.5 mM EDTA and a plate size of 100 × 100 mm. The relative amounts of free and bound RNAs were determined by using the gel analysis system FLA-2000G.

Gel Shift Assay for Peptides—Prior to gel shift assay with PAGE, samples were mixed in a binding buffer containing 30 mM sodium phosphate buffer (pH 6.9) and 50 mM NaCl, and incubated at 4°C for 30 min. Concentrations of the samples in the binding buffer were 0.05 mM for the RNA and 0–1 mM for each peptide. The peptide-bound RNA was separated from free RNA by 10% PAGE with a condition of acrylamide:bis = 19:1, 45 mM Tris–borate (pH 8.3), 1 mM EDTA. The electrophoresis was performed for 90 min at 100 V/cm with a plate of 100 × 100 mm under the ambient temperature of 4°C. After the electrophoresis, the gels were stained with Toluidinblau O (Chroma Gesellschaft Schmidt & Co.) to visualize RNA containing bands.

NMR Measurements—RNA samples in 30 mM sodium phosphate buffer (pH 6.9) containing 50 mM NaCl were concentrated to 0.1–0.9 mM by ultrafiltration. Peptide samples were dissolved in 30 mM sodium phosphate buffer (pH 6.9) containing 50 mM NaCl. NMR spectra were recorded on a DRX-500 or DRX-600 spectrometer (Bruker) at probe temperatures of 22–32°C. Signals of the exchangeable protons were assigned by using the 2D NOESY spectrum measured in H_2O with a mixing time of 250 ms using the jump-and-return scheme. Signals of non-exchangeable protons were assigned by using the 2D NOESY and 2D TOCSY spectra with mixing times of 300 and 50 ms, respectively. 2D HCCH-COSY and 2D HCCH-TOCSY spectra of the labelled samples were used to assign sugar spin systems (*24*). H2 protons of adenosine were assigned using the 2D HCCH-TOCSY and 2D HSQC spectra of the labelled sample (*25*).

RESULTS

Design of the Model RNAs and RNA Digestion Analyses—According to the results of Qin *et al*., a model RNA, U6–45, was designed for the present study (Fig. 2B). In addition to the RNA with the wild-type sequence, four mutants lacking some or all of the bulge-out residues were constructed, as shown in Fig. 3; each of the three bulged-out regions is deleted in M1-M3, and all of them were deleted in M4. We used fluorescein-labelled RNA for the competitive gel mobility shift assay. Combined with the use of the imaging analyzer, comparable sensitivity is obtained as with the method using radioisotopes.

The secondary structures of the model RNAs are analysed by enzymatic probing with RNase T_1, RNase T_2 and RNase V_1. The digestion patterns are shown in the Supplementary Fig. 1 and the results of digestion analysis are shown in Fig. 3. The UUCG loop region was digested by RNase T_1 and RNase T_2 equally for each RNA, indicating the formation of the loop structure. G7-A10 and A40-A41 in the stem region was digested by RNase V_1 equally for each RNA, indicating the formation of the stem structure. Thus, it was confirmed that each RNA forms the desired hairpin structure, although some differences were found around the bulged-out residues.

For U6–45, the stem between the bulged-out residues was digested weakly by RNase V_1, indicating that the region is flexible. M1 showed a similar digestion pattern with U6–45, except for the region around G12 and U14. This region was digested more than that of U6–45 by RNase V_1, indicating that the stem region became more stable, due to the removal of the bulged-out residue, A13. M2 also showed a similar pattern to that of the wild-type RNA, and again, the stem region was stabilized by the removal of A17. M3 lacking A31-G33 was cleaved by RNase T_2 at U14-A17, whereas RNase V_1 also cleaved the region, suggesting that M3 still forms a similar stem-bulge conformation with U6–45 and M1. In contrast, the analyses indicated that M4 forms a simple hairpin structure.

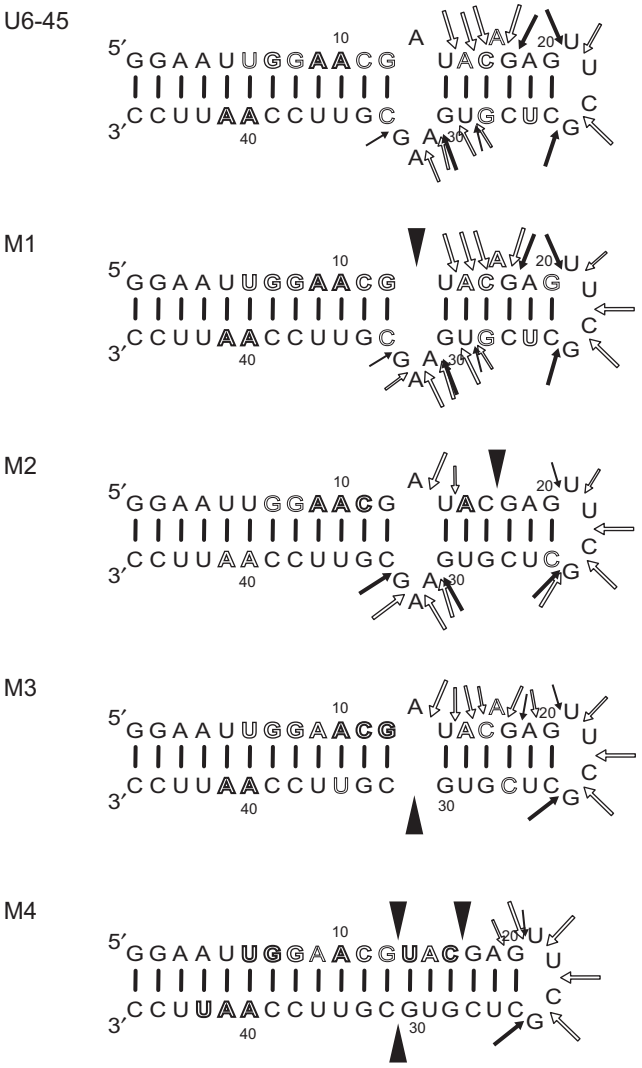

Fig. 3. **Results of RNase digestion analysis summarized on the secondary structures.** Filled and open arrows indicate the sites digested by RNase T_1 and T_2, respectively. Open characters indicate the sites digested by RNase V_1. For all cases, a larger arrow or character indicates stronger digestion. The mutation sites are indicated by arrows.

Binding of NS1 Protein to Model RNAs—To compare the binding affinities of the model RNAs to the NS1 protein, a competition assay was performed. The results of the self-competition assay using non-labelled U6–45 as competitor and fluorescein-labelled U6–45, are shown in Fig. 4. With the addition of the competitor RNA, the amount of labelled U6–45 in the complex was decreased, indicating that the competition works well. In contrast, with the addition of M1, lacking a bulged-out residue, the U6–45 complex could be observed even with a high concentration of the competitor RNA, indicating that M1 has lower affinity to the NS1 protein than U6–45 (Fig. 4B). This was also found for M3, as shown in Fig. 4D. M2, lacking the single bulged-out residue, also showed weak inhibition (Fig. 4C). However, M4 competed as well as U6–45 (Fig. 4E). Clearly, M4 recovers the NS1 binding affinity and M2 showed weaker binding, as compared to U6–45 and M4. From the analysis in Fig. 4, the dissociation constants for U6–45 and M4 to the NS1 protein were both estimated to be 2×10^{-9} M. The ratio of complex and free-labelled RNAs is summarized in the Supplementary Fig. 2.

Design of Peptide Derived from NS1 Protein and Gel Shift Assay—The RNA binding domain of NS1 protein consists of three α-helices as shown in Fig. 1A. Helix-1, -2 and -3 contain 2, 6 and 3 basic amino acid residues, respectively, and the basic amino acid residues except for Arg19, located in the helix-1, are exposed to solvent in the structures of NS1(1–73) (*18*, *19*). Thus, it is expected that the helix-2 is responsible for the RNA binding. This is consistent with the fact that Arg38 and Lys41 located in the helix-2 are involved in direct RNA binding (*26*). Accordingly, a peptide, NS1–2, derived from the helix-2 was constructed. The other peptide, NS1–3, derived from helix-3, was also constructed as a reference. In order to increase the water solubility, hydrophobic residues located inside of the NS1 protein were replaced by alanine residues in the designed peptides as show in Fig. 1B. Both of helix-2 and -3 are amphiphilic and the replaced leucine and isoleucine residues are located in the hydrophobic side of the helices (Supplementary Fig. 3). Both peptides showed enough water solubility to be used even for the NMR measurements. None of αH proton signals were observed in the lower magnetic field

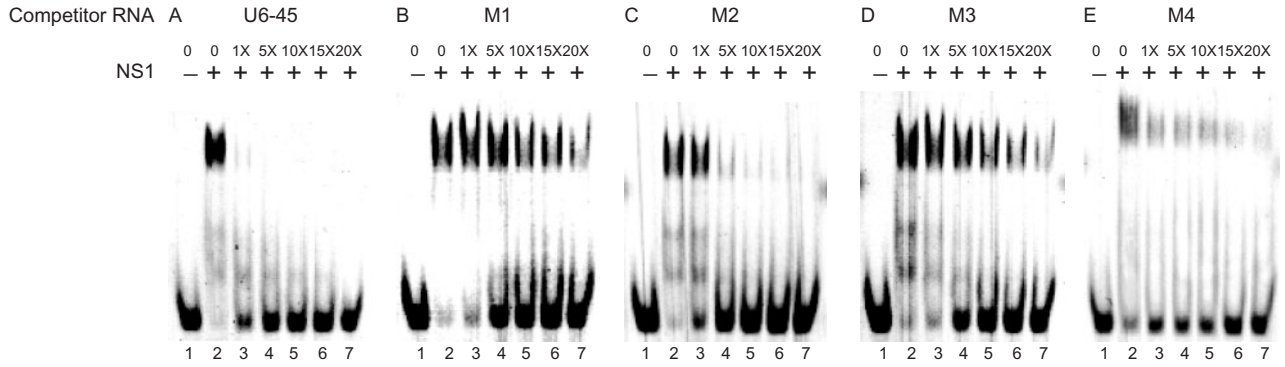

Fig. 4. **Competitive gel shift assay.** Each lane contains 0.05 μM of U6–45. Lanes 2–7 each contain 0.12 μM of NS1 protein. Lanes 3–7 contain 0.05, 0.25, 0.5, 0.75 and 1.0 μM of competitor RNA, respectively. The competitor RNAs are indicated for each panel.

than the signal of water (data not shown), suggesting that two peptides do not form a β strand. The free peptides might form a random coil structure because no NOEs indicating the formation of the α-helix were observed.

A shorter model RNA consisting of 34 nucleotide residues, U6–34, was designed for NMR measurements (Fig. 2C). The conformation of the model RNA was confirmed to be the predicted hairpin structure by PAGE and NMR analyses as described below. Binding of the peptides to the model RNA, U6–34, was analysed by the gel shift assay and the result was shown in Fig. 5. It is noted that no band corresponding to the dimer duplex was observed for the free RNA (Lane 1). By adding NS1–2, the band of U6–34 in the free state was decreased and the band of U6–34 in the complex was observed, indicating that NS1–2 binds to U6–34 (Lanes 2–4). The band of the complex was smear due to the dissociation of the peptide during the run, indicating the affinity is weak. In contrast, NS1–3 did not bind to U6–34 (Lanes 5–7). Thus, it is clearly confirmed that the helix-2 of NS1 protein is responsible for the RNA binding at least for the U6 snRNA. The free RNA band was still observed in the lane 2 in Fig. 5, containing 0.05 mM of RNA and 0.25 mM of peptide and the dissociation constant was estimated to be 10^{-4}–10^{-5} M.

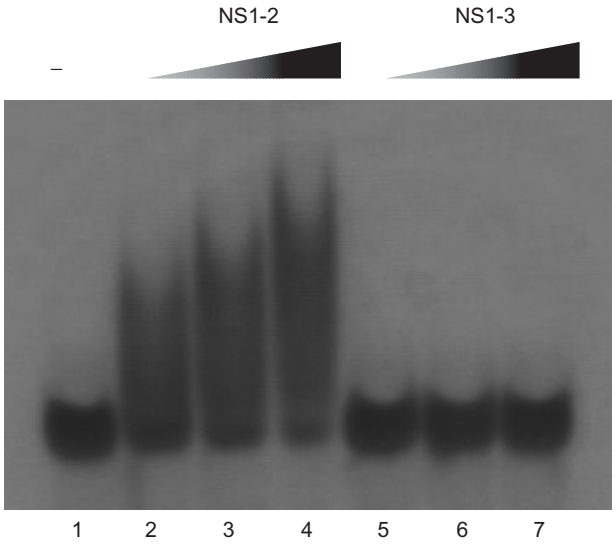

Fig. 5. **Gel shift assay for the RNA-binding ability of the peptides.** RNA samples were analysed by non-denaturing PAGE. The concentration of RNA was 0.05 mM for each lane in 5 μl of the loading buffer. Lane 1 is RNA alone. Lanes 2–4 (5–7) contain 0.25, 0.5 and 1.0 mM of NS1–2 (NS1–3).

NMR Analysis of U6–34—In order to elucidate the NS1–2 recognition site of U6–34, we conducted NMR experiments. Imino proton signals were assigned by using the 2D NOESY spectrum. NMR signals of H5/H6 of pyrimidine and H8 of purine, and ribose H1′ protons of U6–34 were assigned with the conventional method (*27*) by mainly using the 2D NOESY and 2D TOCSY spectra. Semi-selective [^{13}C/^{15}N] RNAs were used to confirm the assignment especially for residues in the bulge-out region.

The bottom spectrum of Fig. 6A corresponds to the free RNA and characteristic signals for the UUCG loop were observed at 11.5 and 10.4 ppm (*28*), indicating that U6–34 forms the desired hairpin structure. For each of G7 and G8, two imino proton signals were observed due to heterogeneity of the 3′ terminal which commonly happens in the transcription reaction with the T7 RNA polymerase. Sharp imino proton signals were not

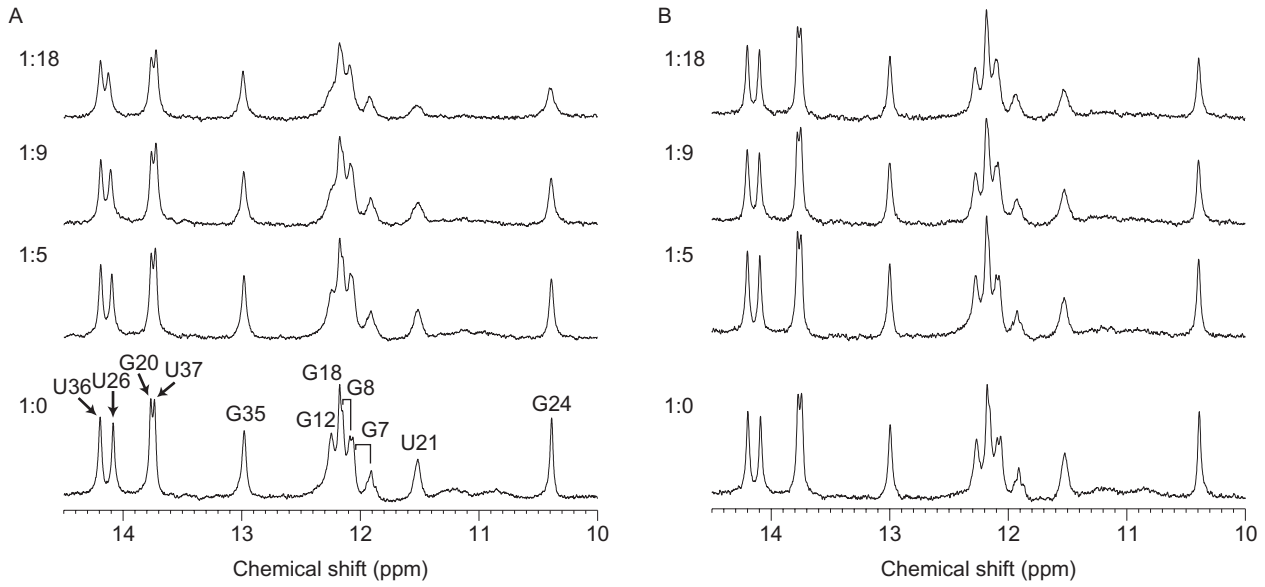

Fig. 6. **Peptide titration of imino proton spectra of U6–34.** The concentration of U6–34 was 0.1 mM and the molar ratios of U6–34 and NS1–2 (A) or NS1–3 (B) were indicated for each row. The signal assignments are shown in the bottom row of (A). A total of 600 MHz ^{1}H-NMR spectra were measured at a probe temperature of 22°C. For each experiment, 400 of scans were accumulated and 3.0 Hz of line broadening was applied prior to the Fourier transformation.

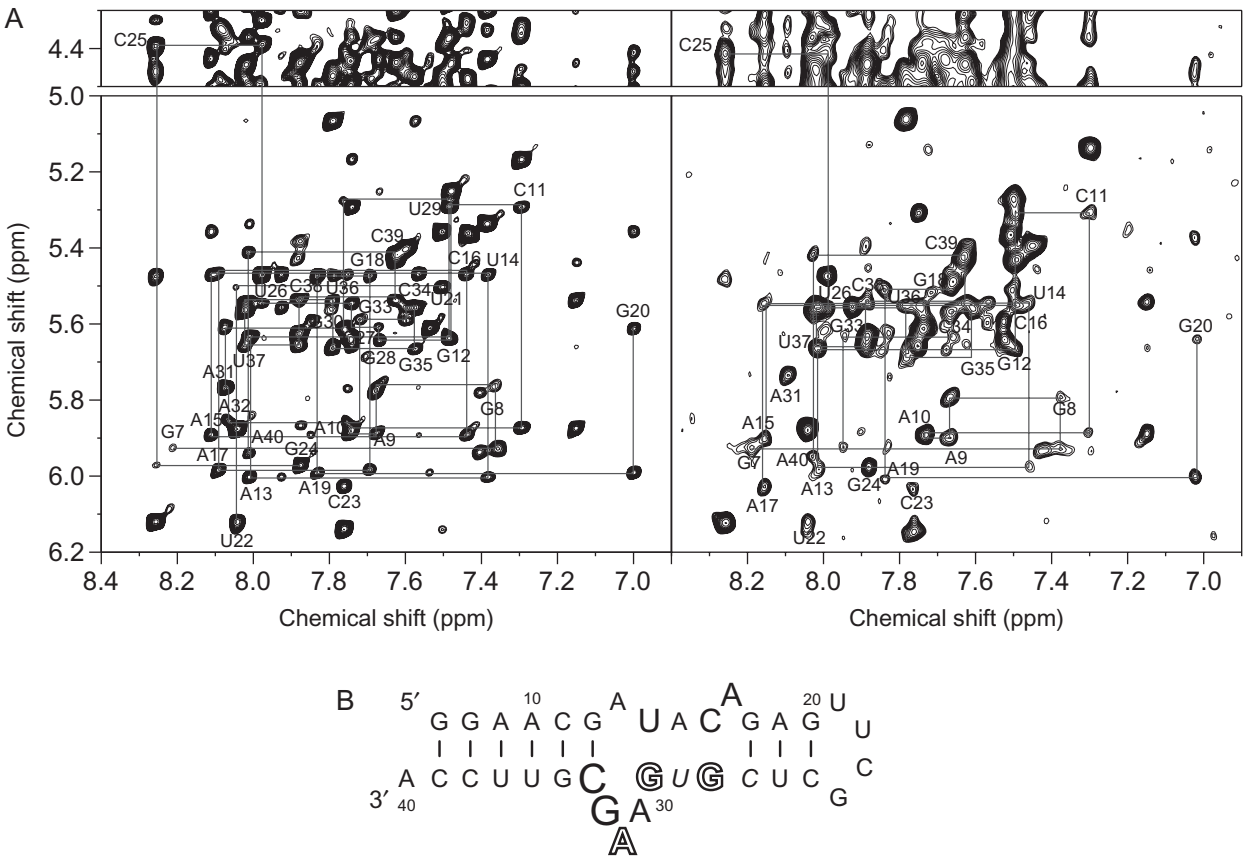

Fig. 7. **Chemical shift perturbation of U6–34 upon binding of NS1–2.** For the complex, the concentrations of U6–34 and NS1–2 were 0.1 and 1.8 mM, respectively. (A) 2D NOESY spectra of U6–34 in the absence (left) and presence (right) of NS1–2. The NOE connectivity is depicted by lines. The residue number labels indicate intra residue H6/H8-H1′ cross peaks. (B) Mapping of the chemical shift change on the secondary structure. Medium characters indicated the residues whose chemical shifts were changed by 0.05–0.1 ppm. Large characters indicated the residues with chemical shift changes of 0.1 ppm or more. Open large characters indicated the residues with large shifts or disappearances. Italic fonts indicate the residues that could not be assigned in the complex.

observed for the regions including residues U14-C16 and G28-G30 between the bulge-out residues. The NOE between H2 of A15 and H1′ of G30 which is the typical NOE for a regular A-type stem was not observed, whereas the NOEs between H2 of A31 and H1′ of C16 as well as H2 of A32 and H1′ of A15 were observed, suggesting the interaction between A31 and A15 as well as A32 and U14. Thus it was indicated that the regular A-type stem structure is not formed in this region as shown in Fig. 2C.

NMR Analysis of Interaction between NS1–2 and U6–34—By adding the NS1–2 to U6–34, most imino proton signals including G12, G18, G20, U21, G24 and U26 were broadened and some signals including U26 were slightly, by less than 0.1 ppm, shifted (Fig. 6A). In contrast, addition of NS1–3 did not change the imino proton signals (Fig. 6B). These results are consistent with that of the gel shift assay: NS1–2 binds to U6–34 but NS1–3 does not. Simultaneously, the results suggest that the NS1–2 binds to the bulge-out region but not to the stems or the UUCG loop. The concentration of the RNA and peptides were 0.1 and 1.8 mM, respectively, for the top spectrum of Fig. 6A, which were higher than those for lane 4 in Fig. 5, indicating that most of the RNA forms the complex.

We further analysed the effect of NS1–2 on the NMR signals of U6–34. Figure 7A shows the difference of the NOESY spectra of U6–34 in the absence (left) and presence (right) of NS1–2. For the spectra with NS1–2, the concentration of the RNA and peptides were 0.1 and 1.8 mM, respectively. Most of non-exchangeable proton signals were not changed upon addition of NS1–2 except for signals due to residues U14-A17 and G28-C34. Signals due to G33 shifted by more than 0.1 ppm and, furthermore, signals due to H8 and H1′ of G28 and G30 and H8 signal of A32 could not be assigned in the complex due to a large shift or disappearance. Residues G28-C34 showed a larger shift or broadening than residues U14-A17. These results were summarized in Fig. 7B and it was found that NS1–2 binds to the bulge-out region including the residues U14-A17 and G28-C34. It is noted that H1′ signals of C27 or U29 were not assigned in the complex due to an overlap with other signals.

DISCUSSION

RNA–protein interactions are important in many cellular processes. Recent structural studies of RNA–protein complexes have revealed that many specific contacts

are made between amino acids and nucleotides (*29*). In some cases, small peptides derived from RNA binding proteins such as Rev and Tat can recognize the specific sequence/structure of RNA molecules. Human immunodeficiency virus type-1 Rev peptide, consisting of 23 amino acids, forms an α-helix and recognizes an internal loop region of RRE RNA (*30*). Bovine immunodeficiency virus Tat peptide, consisting of 14 amino acids, forms a β-turn and recognizes dsRNA with bulge-out residues playing major roles (*31*). These small peptides provided excellent model systems for structural analysis of RNA–protein interaction by NMR spectroscopy. A detailed structural understanding of the interactions in the complex may assist in the design of therapeutics for viral disease.

Most RNA-binding proteins bind to their specific RNA by recognizing its characteristic structure; the HIV Tat protein specifically recognizes TAR RNA, and the HIV Rev protein recognizes the RRE (*30–32*). In contrast, the NS1 protein recognizes several kinds of RNAs, as described above. Thus, it is interesting to elucidate how such a small protein recognizes different kinds of RNAs. Since the NS1 protein weakly and non-specifically binds to RNAs, we used a competitive gel shift assay, rather than a simple gel shift assay, to analyse the specific RNA binding by the NS1 protein, which clearly revealed the different specificities of the NS1 protein for two kinds of RNAs, RNA containing a bulge and dsRNA. Before performing the competitive gel shift assay, we checked the conformations of the prepared RNA samples. The structural probing experiment showed that the stem-bulge region of the model RNAs designed in this study formed the expected secondary structures.

The competition assay showed that the deletion of each bulged-out region, A13 or A31-G33, decreased the binding affinity to the NS1 protein, suggesting that these residues are required for the NS1 protein binding. A17 is less important for the binding than A13 and A31–33, but is still required for efficient binding. Although it is not clear which residue directly interacts with the NS1 protein, we would expect that the specific structure of U6–45 is required for recognition by the NS1 protein. On the other hand, the simultaneous deletion of all of the bulged-out residues restored the binding affinity. Although the NS1 protein binding to dsRNA has already been documented (*12*, *13*), the fact that dsRNA competes with U6–45 for the NS1 protein binding is important. Together with the fact that the RNA binding domain of the NS1 protein is as small as about 70 residues, even though it forms a dimer, the NS1 binding sites for U6 snRNA and dsRNA seem to be identical or, at least, overlapped. This is consistent with the fact that the Arg38 and Lys41 residues, located in helix 2 of the NS1 protein, are involved in the interaction with U6 snRNA and dsRNA (*26*). It was also indicated that M1, M2 and M3, as well as U6–45, were not recognized as dsRNAs. Probably, the double-stranded part of U6–45 is too short to be recognized as dsRNA by the NS1 protein. In fact, Yin *et al*. recently showed the structural model of NS1-dsRNA complex in which 16bp RNA is recognized by the protein (*33*). The weak affinity of M1, M2 and M3 for the NS1 protein might be due to the similar conformation of U6–45, with its shorter double-stranded region, or to non-specific affinity.

The NS1 protein binds to poly(A) and influenza viral RNA, as described above. Hatada *et al*. suggested that the A bulge, in a double helix in viral RNA, is the NS1 binding site (*15*). A common feature of the three RNAs, poly(A), viral RNA and U6 snRNA, is the stretch of 'bulged-out' A residues with a specific spatial arrangement. Therefore, we can conclude that the NS1 protein recognizes either the stretch of 'bulged-out' A residues or dsRNA.

Two peptides consisting of 18 amino acid residues were designed and their RNA binding activities were analysed. Both helices-2 and -3 of NS1 proteins are amphiphilic and the leucine and isoleucine residues are located on the hydorophobic side of the helices and we replaced some of the hydrophobic residues to increase the water solubility (Supplementary Fig. 3). Because these hydrophobic residues are located inside of the protein in the structures of the RNA binding domain of NS1 protein (*18*, *19*), the replacements were expected to be silent for the RNA binding activity. As expected, NS1–2 containing six basic residues bound to U6–34, whereas NS1–3 containing three basic residues did not. Probably, three basic residues are too few to have an effective RNA binding activity. In fact, the Rev and Tat peptides contain 11 basic residues out of 23 residues and 7 out of 14, respectively (*30*, *31*).

A chemical shift perturbation technique is often used to observe the interaction between two biomolecules. The surface of the molecule that is interactive can be confirmed by the change of the NMR signal. However, the signals are changed even by the influence of the structural change caused by the formation of the complex. Thus, great care must be taken to interpret the interaction-induced chemical shift perturbation. It should be noted that Spitzfaden *et al*. (*34*) have shown that although perturbed resonances give good initial estimates of a binding surface, the effects extend beyond the direct contact area. The most likely explanation of the results of the chemical shift perturbation analysis in this study is that the NS1–2 binding site of U6–34 is mainly the RNA strand consisting of G28-C34 in the bulge-out region, including the bulged A31 and A32. The structure of the opposite strand consisting of U14-A17 might be changed upon the binding. Probably, NS1–2 binds to the major groove side of the bulge-out region as is the case with other arginine-rich peptides such as Rev and Tat. NS1–2 might form α-helix upon binding to U6–34 due to its amphiphilic nature. The observed broadenings of imino proton resonances corresponding to the base pairs adjacent to the bulge-out region, G12-C34 base pair, are probably due to the NS1–2 binding to the bulge-out region. The imino proton signals due to U21 and G24 of the UUCG loop also broadened upon binding of NS1–2. This is probably due to the partial disruption of the stem consisting of G18-G20 and C25-C27 upon binding of NS1–2 to the adjacent bulge-out region.

In conclusion, it was shown that the NS1 protein recognizes either the stretch of 'bulged-out' A residues or dsRNA. Further, NS1–2 peptide binds to G28-C34 in the bulge-out region of U6-34, including the bulged A31 and A32, suggesting that NS1 protein also bind to the 'bulged-out' A residues in a similar manner.

Supplementary data are available at *JB* online.

We thank Dr S. Nakada (Yamanouchi Pharmaceutical Co.) for advice and for providing the plasmid encoding NS1 protein, and Drs E. Hatada and R. Fukuda (Kanazawa University Graduate School of Medical Science) for giving us NS1 protein samples. We thank Dr K. Takai and Mr R. Ouchi for a kind gift of T7 RNA polymerase and Drs T. Sakamoto and N. Nameki for critical readings of the manuscript. This work was supported by 'Research for the Future' Program (JSPS-RFTF97L00503) from the Japan Society for the Promotion of Science and by a Grant-in-Aid for High Technology Research from Ministry of Education, Science, Sports and Culture, Japan.

REFERENCES

1. Buonagurio, D.A., Nakada, S., Parvin, J.D., Krystal, M., Palese, P., and Fitch, W.M. (1986) Evolution of human influenza A viruses over 50 years: rapid, uniform rate of change in NS gene. *Science* **232**, 980–982
2. Norton, G.P., Tanaka, T., Tobita, K., Nakada, S., Buonagurio, D.A., Greenspan, D., Krystal, M., and Palese, P. (1987) Infectious influenza A and B virus variants with long carboxyl terminal deletions in the NS1 polypeptides. *Virology* **156**, 204–213
3. Suarez, D.L. and Perdue, M.L. (1998) Multiple alignment comparison of the non-structural genes of influenza A viruses. *Virus Res.* **54**, 59–69
4. Nemeroff, M.E., Qian, X.-Y., and Krug, R.M. (1995) The influenza virus NS1 protein forms multimers in vitro and in vivo. *Virology* **212**, 422–428
5. Qian, X.-Y., Chien, C.-Y., Lu, Y., Montelione, G.T., and Krug, R.M. (1995) An amino-terminal polypeptide fragment of the influenza virus NS1 protein possesses specific RNA-binding activity and largely helical backbone structure. *RNA* **1**, 948–956
6. Qian, X.-Y., Alonso-Caplen, F., and Krug, R.M. (1994) Two functional domains of the influenza virus NS1 protein are required for regulation of nuclear export of mRNA. *J. Virol.* **68**, 2433–2441
7. Aragón, T., de la Luna, S., Novoa, I., Carrasco, L., Ortín, J., and Nieto, A. (2000) Eukaryotic translation initiation factor 4GI is a cellular target for NS1 protein, a translational activator of influenza virus. *Mol. Cell. Biol.* **20**, 6259–6268
8. Qiu, Y. and Krug, R.M. (1994) The influenza virus NS1 protein is a poly(A)-binding protein that inhibits nuclear export of mRNAs containing poly(A). *J. Virol.* **68**, 2425–2432
9. Lu, Y., Qian, X.-Y., and Krug, R.M. (1994) The influenza virus NS1 protein: a novel inhibitor of pre-mRNA splicing. *Genes & Dev* **8**, 1817–1828
10. Qin, Y., Nemeroff, M., and Krug, R.M. (1995) The influenza NS1 protein binds to a specific region in human U6 snRNA and inhibits U6-U2 and U6-U4 snRNA interactions during splicing. *RNA* **1**, 304–316
11. Wang, W. and Krug, R.M. (1998) U6atac snRNA, the highly divergent counterpart of U6 snRNA, is the specific target that mediates inhibition of AT-AC splicing by the influenza virus NS1 protein. *RNA* **4**, 55–64
12. Hatada, E. and Futada, R. (1992) Binding of influenza A virus NS1 protein to dsRNA in vitro. *J. Gen. Virol.* **73**, 3325–3329
13. Lu, Y., Wambach, M., Katze, M.G., and Krug, R.M. (1995) Binding of the influenza virus NS1 protein to double-stranded RNA inhibits the activation of the protein kinase that phosphorylates the elF-2 translation initiation factor. *Virology* **214**, 222–228
14. Min, J.Y. and Krug, R.M. (2006) The primary function of RNA binding by the influenza A virus NS1 protein in infected cells: Inhibiting the 2′-5′ oligo (A) synthetase/RNase L pathway. *Proc. Natl. Acad. Sci. USA* **103**, 7100–7105
15. Hatada, E., Saito, S., Okishio, N., and Fukuda, R. (1997) Binding of the influenza virus NS1 protein to model genome RNAs. *J. Gen. Virol* **78**, 1059–1063
16. Marlón, R.M., Aragón, T., Belose, A., Nieto, A., and Ortín, J. (1997) The N-terminal half of the influenza virus NS1 protein is sufficient for nuclear retention of mRNA and enhancement of viral mRNA translation. *Nucleic Acids Res.* **25**, 4271–4277
17. Park, Y.W. and Katze, M.G. (1995) Translational control by influenza virus. Identification of cis-acting sequences and trans-acting factors which may regulate selective viral mRNA translation. *J. Biol. Chem* **270**, 28433–28439
18. Chien, C.-Y., Tejero, R., Huang, Y., Zimmerman, D.E., Ríos, C.B., Krug, R.M., and Montelione, G.T. (1997) A novel RNA-binding motif in influenza A virus non-structural protein 1. *Nature Struc. Biol.* **4**, 891–895
19. Liu, J., Lynch, P.A., Chien, C.-Y., Montelione, G.T., Krug, R.M., and Berman, H.M. (1997) Crystal structure of the unique RNA-binding domain of the influenza virus NS1 protein. *Nature Struc. Biol.* **4**, 896–899
20. Kramer, A. (1996) The structure and function of proteins involved in mammalian pre-mRNA splicing. *Annu. Rev. Biochem.* **65**, 367–409
21. Harada, F., Kato, N., and Nishimura, S. (1980) The nucleotide sequence of nuclear 4.8S RNA of mouse cells. *Biochem. Biophys. Res. Commun.* **95**, 1332–1340
22. Rinke, J., Appel, B., Digweed, M., and Lührmann, R. (1985) Localization of a base-paired interaction between small nuclear RNAs U4 and U6 in intact U4/U6 ribonucleoprotein particles by psoralen cross-linking. *J. Mol. Biol.* **185**, 721–731
23. Young, J.F., Desselberger, U., Palese, P., Ferguson, B., Shatzman, A.R., and Rosenberg, M. (1983) Efficient expression of influenza virus NS1 nonstructural proteins in *Escherichia coli*. *Proc. Natl. Acad. Sci. USA* **80**, 6105–6109
24. Pardi, A. and Nikonowicz, E.P. (1992) Simple procedure for resonance assignment of the sugar protons in ^{13}C labeled RNA. *J. Am. Chem. Soc.* **114**, 9202–9203
25. Legault, P., Farmer, B.T., II., Mueller, L., and Pardi, A. (1994) Through-bond correlation of adenine protons in a ^{13}C-labeled ribozyme. *J. Am. Chem. Soc.* **116**, 2203–2204
26. Wang, W., Riedel, K., Lynch, P., Chien, C.-Y., Montelone, G.T., and Krug, R.M. (1999) RNA binding by the novel helical domain of the influenza virus NS1 protein requires its dimer structure and a small number of specific basic amino acids. *RNA* **5**, 195–205
27. Wüthrich, K. (1986) *NMR of Proteins and Nucleic Acids* John Wiley & Sons. Inc., New York
28. Varani, G., Chenog, C., and Tinoco, I., Jr. (1991) Structure of an unusually stable RNA hairpin. *Biochem.* **30**, 3280–3289
29. Frankel, A.D. (2000) Fitting peptides into the RNA world. *Curr. Opin. Stuct. Biol.* **10**, 332–340
30. Battiste, J.L., Mao, H., Rao, N.S., Tan, R., Muhandiram, D.R., Kay, L.E., Frankel, A.D., and Williamson, J.R. (1996) Alpha helix-RNA major groove recognition in an HIV-1 rev peptide-RRE RNA complex. *Science* **273**, 1547–1551
31. Puglisi, J.D., Chen, L., Blanchard, S., and Frankel, A.D. (1995) Solution structure of a bovine immunodeficiency virus Tat-TAR peptide-RNA complex. *Science* **270**, 1200–1203
32. Ye, X., Kumar, R.A., and Patel, D.J. (1995) Molecular recognition in the bovine immunodeficiency virus Tat peptide-TAR RNA complex. *Chem. Biol.* **12**, 827–840

33. Yin, C., Khan, J.A., Swapna, G.V.T., Ertekin, A., Krug, R.M., Tong, L., and Montelione, G.T. (2007) Conserved surface features form the double-stranded RNA binding site of non-structural protein 1 (NS1) from influenza A and B viruses. *J. Biol. Chem.* **82**, 20584–20592

34. Spitzfaden, C., Weber, H.P., Braun, W., Kallen, J., Wider, G., Widmer, H., Walkinshaw, M.D., and Wüthrich, K. (1992) Cyclosporin A-cyclophilin complex formation. A model based on X-ray and NMR data. *FEBS Lett.* **300**, 291–300